Original Research

Improved clearance of radioiodinated hypericin as a targeted anticancer agent by using a duodenal drainage catheter in rats

Marlein Miranda Cona[1,2], Yuanbo Feng[1,2], Alfons Verbruggen[3], Raymond Oyen[1] and Yicheng Ni[1,2]

[1]Department of Imaging & Pathology, Faculty of Medicine, Biomedical Sciences Group, KU Leuven, Herestraat 49, Leuven, Belgium; [2]Molecular Small Animal Imaging Centre/MoSAIC, Faculty of Medicine, Biomedical Sciences Group, KU Leuven, Herestraat 49, Leuven, Belgium; [3]Faculty of Pharmaceutical Sciences, Biomedical Sciences Group, KU Leuven, Herestraat 49, Leuven, Belgium
Corresponding author: Yicheng Ni. Email: yicheng.ni@med.kuleuven.be

Abstract

We sought to reduce the radioactive intestinal waste after intravenous injection of necrosis avid iodine-131-labeled hypericin in dual-targeting anticancer radiotherapy and to study its pharmacokinetics in rats using a newly designed catheter. Iodine-123-labeled hypericin was prepared with iodogen as oxidant and characterized by high-performance liquid chromatography and mass spectrometry. After iodine-123-labeled hypericin administration, duodenal juice was collected via a catheter from groups of rats ($n = 5$) at intervals of 0–4, 4–8 or 20–24 h. The content was assessed by gamma-counting. The biodistribution and pharmacokinetics of iodine-123-labeled hypericin were investigated in rats without ($n = 5$) and with continuous catheterization ($n = 5$) for 9 h. After labeling, a high radiochemical yield was obtained with iodine-123-labeled hypericin (>95%), as confirmed by high-performance liquid chromatography and mass spectrometry. In the duodenal aspirate from animals with intermittent catheterization during 24 h, radioactivity accounted for 46% of the total with two peaks at 3 h and 8 h, suggesting enterohepatic circulation. Rats with 9 h of catheterization exhibited one peak representing 20% of the radioactivity. Major metabolites appeared to be conjugated iodine-123-labeled hypericin forms. In rats without and with catheter, iodine-123-labeled hypericin showed exponential elimination from plasma with no significant dehalogenation. Delayed iodine-123-labeled hypericin excretion, a higher maximum concentration (C_{max}), larger area under concentration-time curve [$AUC_{(0-\infty)}$] and a longer mean residence time were observed in non-catheterized animals ($P < 0.05$). The catheterized group exhibited lower urinary excretion than non-catheterized group ($P < 0.05$). Rats with a catheter showed lower radioactivity ($P = 0.01$) in the small intestines than those without a catheter (1.82 ± 0.41 versus 18.95 ± 4.32 percentage of the injected dose). After iodine-123-labeled hypericin administration, the radioactivity excreted into bile was efficiently removed from the body via a duodenal catheter. Radiation overexposure due to the prolonged elimination of iodine-131-labeled hypericin can be prevented using this approach.

Keywords: Iodine-123-labeled hypericin, catheter, pharmacokinetics, biodistribution, cancer, bile

***Experimental Biology and Medicine* 2013; 238: 1437–1449. DOI: 10.1177/1535370213508235**

Introduction

Cancer remains a lethal disease, with limited curative options. OncoCiDia is a generic dual-targeting anticancer approach intended as a complementary modality to improve the treatability of most solid tumors.[1] Based on a soil-to-seeds principle, OncoCiDia selectively radiocontaminates the neoplastic microenvironment (soil) to eradicate the adjacent cancer cells (seeds). It consists of overnight-consecutive intravenous administrations of two natural derivatives with pre-identified high, diverse but synergetic targetability, i.e. a vascular disrupting agent (e.g. combretastatin A4 phosphate or CA4P) and a necrosis avid compound (e.g. iodine-131-labeled hypericin or ^{131}I-Hyp).

CA4P is a prodrug of combretastatin A4 (CA4) extracted from the African bush willow. Upon intracellular uptake, CA4P is metabolized into active CA4 that binds and destabilizes the cytoskeleton tubulin of the immature tumor endothelium, leading to obstruction of the intratumoral microcirculation and subsequent tumor necrosis.[2,3] Hypericin (Hyp) is a naturally occurring compound isolated from hypericum perforatum (St. John's Wort), which has been exploited as an herbal medicine for over a century in the treatment of different disorders.[4,5] Iodine-131 (^{131}I) is a beta-emitter that has been the first choice for treating

thyroid cancer. Because of its half-life (8.02 days) and decay mode (maximum beta energy: 606 KeV; abundance: 89.6%), ^{131}I causes mutational changes and death in the tumor cells containing it (self-dose effect) or nearby cells up to a distance of some millimeters (crossfire effect). By electrophilic substitution of one of the hydrogen atoms on the Hyp aromatic ring with a ^{131}I atom, ^{131}I-Hyp can be easily obtained. This radioactive agent has been discovered to have a high avidity for necrotic tissues as well as being retained long.[6,7]

By means of two consecutive intravenous injections with OncoCiDia, CA4P first creates the specific necrosis target for ^{131}I-Hyp, which then acts as a cleansing shot to wipe out the residual tumor cells by cross-fire beta radiation.[1] Significant tumor shrinkage and growth delay have been observed in animals with different allograft tumor models after a single treatment.[8–10]

However, the use of radiation for cancer therapy also causes the exposure of healthy tissues to the treatment and the related adverse effects of this.[11] Previous biodistribution studies reported that radioiodinated Hyp was mainly metabolized through the hepatobiliary pathway, with high levels of radioactivity found in the intestines within two days of the injections.[12,13] Accordingly, dosimetry calculations have identified the intestinal wall as the dose-limiting organ due to the high radiation dose deposited on it. One of the main concerns over radiation exposure of the intestinal tract is the occurrence of acute gastrointestinal (GI) syndrome, which has been traditionally attributed to the direct ionizing radiation damage of the intestinal epithelia.[14] In this study, we designed a device for duodenal juice drainage in rodents by modifying a commercial Foley catheter, which is used in patients with acute urinary retention. By doing this, we intended to explore the suitability of this approach to constantly withdraw the radioactivity excreted from the hepatobiliary route into the intestines and to minimize the radiation overexposure in patients undergoing OncoCiDia treatment. For this purpose, we determined the percentage of radioactivity in the duodenal fluids over time in pre-catheterized animals. In addition, we evaluated the impact of such a balloon catheter on the pharmacokinetics and biodistribution of radioiodinated Hyp by comparing animals without and with the catheter.

Technically based on the known similarity of iodine isotopes, identity confirmation of the intact iodine-123-labeled hypericin (^{123}I-Hyp) in stock solutions and biological medium was confirmed with iodine-127-labeled hypericin (^{127}I-Hyp) as a standard. For radioprotection purpose, the biodistribution and pharmacokinetic experiments were performed using the gamma-emitter Iodine-123 (^{123}I) with a half-life of 13.2 h, as surrogate of ^{131}I with a half-life of 8.02 days and higher energy.

Materials and methods

Tracer preparation and characterization

Hypericin (1, 3, 4, 6, 8, 13-Hexahydroxy-10, 11-dimethylphenanthro-[1, 10, 9, 8-opqra] perylene-7, 14-dione or Hyp) with a purity greater than 98% was obtained from (Planta Natural Products, Wien, Austria; http://www.planta.at/hyper/hyper.htm).

Hyp was radiolabeled with sodium iodide (^{123}I-NaI) (GE Healthcare, Diegem, Belgium) by using Iodogen (1,3,4,6-tetrachloro-3alpha,6alpha-diphenylglucoluril, Sigma Chemical Co., St Louis, MO, USA) as an oxidizing agent in 90:10 (v/v) dimethyl sulfoxide (DMSO)/0.5 M sodium phosphate buffer, at pH 7.4 for 30 min.

To determine the radiochemical yield, high-performance liquid chromatography (HPLC) analysis was carried out in a Merck-Hitachi L-6200 Intelligent pump system (Tokyo, Japan) coupled with a XTerra® C18 analytical column, 4.6 μm, 5 mm × 150 mm (Waters Corporation, Milford, MA, USA), a Merck-Hitachi L-4200 HP UV/VIS detector (Tokyo, Japan) at 254 nm connected in series with a Raytest radioactivity detector (Straubenhardt, Germany). Sample injection was performed through a Rheodyne injector model 7725 valve incorporating a 20 μL fixed loop. The column was eluted with acetonitrile/0.05 M ammonium acetate buffer pH 7.0 in gradient mode (0 min: 5:95 v/v, 25 min: 95:5 v/v, 30 min: 5:95 v/v); at a flow rate of 1.0 mL/min. Acquisition and processing of data were done using GinaStar acquisition software (version 4.6; Raytest, Straubenhardt, Germany).

Since radiopharmaceutical chemistry uses very small amount of substances making difficult sample analysis by UV-HPLC, Hyp was labeled with non-radioactive iodine or iodine-127 (Janssen Chemica, Geel, Belgium) using the procedure mentioned above. A co-injection of 100 kBq of ^{123}I-Hyp with 5 μL of the 20 μg/mL solution of ^{127}I-Hyp was then applied to the column as described above. Comparison between the retention times of the peaks of ^{127}I-Hyp and ^{123}I-Hyp in the UV and radiometric channels were performed. Molecular weight determination of the HPLC-fraction containing ^{127}I-Hyp was carried out by mass measurements in negative ionization mode on a time-of-flight spectrometer (Micromass LCT, Manchester, UK) equipped with an orthogonal electrospray ionization interface and MassLynx™ software. This intended to determine the relation between retention times of ^{123}I-Hyp the in radiometric channel and the reference standard ^{127}I-Hyp of known molecular mass by UV. Hence, the further identification of intact ^{123}I-Hyp in biological samples using HPLC is more accurate by adding a known amount of ^{127}I-Hyp.

The ^{123}I-Hyp was formulated in DMSO/polyethylene glycol 400 (PEG400)/propylene glycol (PG)/water (25:25:25:25, v/v/v/v) and microscopically examined to control aggregates formation.

Animals

In total, 25 Sprague-Dawley rats (Charles River Breeding Laboratories, Inc., St. Aubain les Elbeuf, France) of 10 weeks of age and weighing over 350 g were used. Standard rodent chow (Ssniff Spezialdiäten GmbH, Soest, Germany) and water were given ad libitum. The research protocol was approved by the local Animal Ethics Committee and was according to European Ethics Committee guidelines (decree 86/609/EEC).

Device design

A commercial device Foley catheter consists of a hollow, silicone rubber tube with two concentric lumens. One of its ends contains a solid rubber tip (~5 mm in length) which aid to insert the device into the subject. One lumen is open at the distal end to allow liquid to drain out into a collection bag at the proximal end. The other lumen contains a protective valve near the proximal end and an inflatable balloon at the distal end, which can be filled with saline solution to obstruct the duodenum and to prevent the catheter from slipping out. A plastic guidewire is introduced into the drainage lumen for guiding the catheterization and is removed once the device is in place.

To collect duodenal juices from the rats, 20 Coloplast® Cysto-Care® Folysil® 2-Way Pediatric Silicone Foley Catheters (Humlebæk, Denmark) with balloon volume of 3 mL were modified as follows. The protruding tip of the catheter was excised by 3 mm and a blunt tip was made by sealing the distal opening of the drainage lumen with an electric Bunsen burner (INTEGRA Biosciences AG, Zizers CH-7205, Switzerland). Three new drainage apertures located proximal to the balloon were manually made using a sharp scalpel. At the proximal end of the drainage tube, a 1-mL syringe was connected for fluid collection (Figure 1a).

Catheterization procedure for biliary drainage

The animals were fasted for food but not water overnight before the experiments to empty the stomach and duodenum. After anesthesia with intraperitoneal injection of sodium pentobarbital (Nembutal; Sanofi Sante Animal, Brussels, Belgium) at 40 mg/kg body weight, a midline open abdominal surgery was carried out under sterile conditions. The stomach and duodenal loop were exposed and the common bile duct was identified. With the inserted guidewire, the catheter was introduced via the mouth and advanced down through the esophagus into the stomach (Figure 1b). With the guidewire withdrawn and by hand external maneuver, the catheter was inserted into the

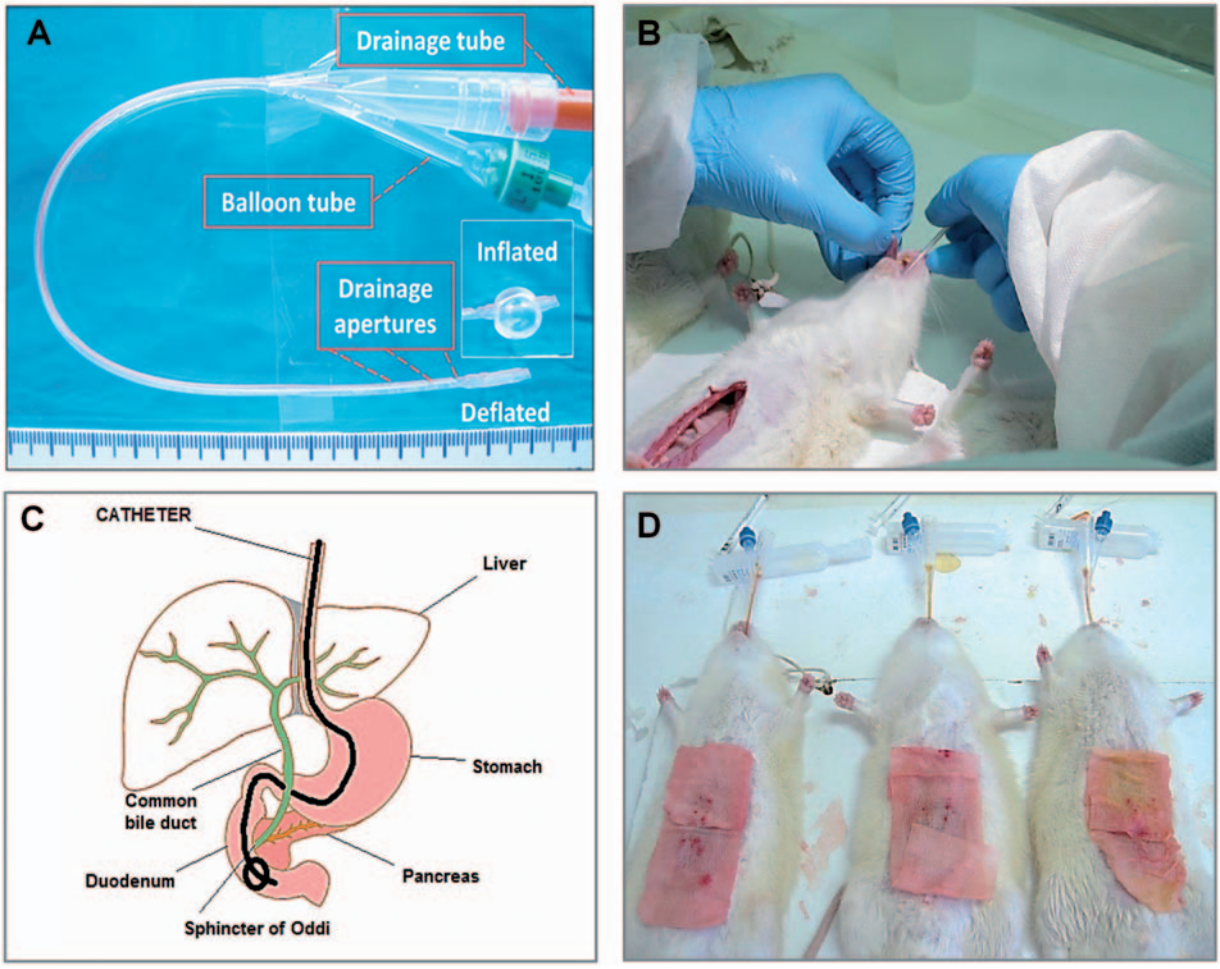

Figure 1 Catheter design and placement for duodenal drainage in rats. (a) Modified from a clinical urinary balloon Foley catheter, the device consists of a tube with two concentric lumens. The distal end of one of the lumens is sealed and three new apertures are made proximal to the inflatable balloon, which is connected to the other lumen with a protective valve at its proximal end. The first lumen allows the fluid drainage through the three apertures into a container connecting to its proximal end. The inflated balloon helps anchor the catheter and block the duodenum. (b) The device is passed via the mouth and advanced down through the esophagus into the stomach. (c) The device is inserted into the second part of the duodenum. After identifying the common bile duct, the balloon and drainage apertures are placed distal to the sphincter of Oddi. (d) Under anesthesia, the duodenal juice is constantly drained and periodically collected while the abdominal incision is covered with saline-moistened gauze.

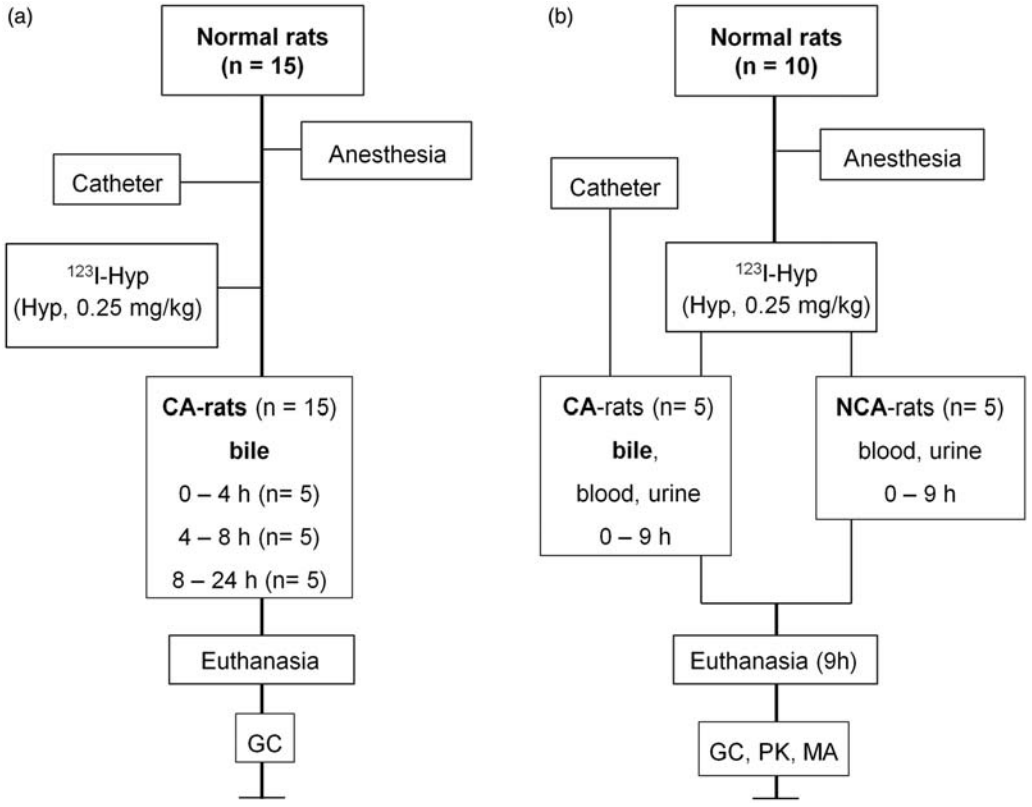

Figure 2 Flow diagram of the experimental protocols. (a) Percentage of radioactivity excreted into the duodenal fluids over time. (b) Impact of the use of the catheter on the pharmacokinetic and biodistribution of radioiodinated Hyp. ^{123}I-Hyp: Iodine-123-labeled iodohypericin; CA: catheterized animals; NCA: non-catheterized animals; GC: gamma counting; PK: pharmacokinetic study; MA: metabolite analysis.

third part of the duodenum, making sure that the balloon and drainage apertures were placed after the sphincter of Oddi. Next, the balloon was inflated with 1.0 mL of saline solution to hold the catheter in place and block the lower gastrointestinal tract (Figure 1c). During the whole procedure, animals were kept under anesthesia and the abdominal incisions were covered with saline-moistened gauze to minimize organ dehydration (Figure 1d).

Collection of duodenal fluids

Fifteen rats were split into three groups of five animals each, receiving a dose of 12.0 MBq of ^{123}I-Hyp intravenously (IV) through the penis vein. One animal group per time interval including 0–4, 4–8 or 20–24 h was subjected to catheter placement and then duodenal juice samples were collected every 1 h. To prevent dehydration, 1.0 mL of saline solution was periodically infused into the abdominal cavity. During the duodenal juice drainage, supplemental anesthetic dose of Nembutal was IP administered to the animals as needed. After fluid collection, the balloon was deflated and the catheter was removed, and the animals were euthanized by an overdose of anesthetics. The samples collected were measured with a 2480 Automatic Gamma Counter, Wizard2TM3'' (Perkin Elmer, USA).

After decay and background corrections, the results were expressed as a percentage of the injected dose (%ID) of ^{123}I-Hyp in duodenal juice, and time-activity curves were then created. Areas under curves ($AUC_{(t-0)}$) were determined with a trapezoidal integration by using the computer program GraphPad Prism version 5.00 for Windows (GraphPad Software Inc., San Diego, USA, www.graphpad.com) (Figure 2a and b).

Duodenal juice collection

Ten rats were split into two groups of five animals each. After the same anesthesia, one group of rats was subject to catheter placement. The remaining rats were set without a catheter as a control group. They were all subjected to an IV injection of 12.0 MBq of ^{123}I-Hyp. From the catheterized rats, samples of duodenal juice were collected every 1 h until a total of 9 h. Thereafter, the samples were counted and subjected to decay and background corrections. Results were expressed as %ID and, time-activity curves were generated. $AUC_{(t-0)}$ were calculated by the trapezoidal integration using the computer program GraphPad Prism version 5.00 for Windows.

Blood and urine sample collection

From animals with and without catheterization, blood samples were collected at 0, 0.25, 0.5, 0.75, 1, 1.5, 2, 2.5, 3, 3.5, 4, 5, 6, 7, 8 and 9 h by cutting a tiny section of the tail each time, and a droplet of Histoacryl® topical skin adhesive (Braun, Tuttlingen, Germany) was applied to stop bleeding. The blood samples were centrifuged and plasma samples were weighed and measured for 1 min using a gamma

counter. Data were expressed as counts per second per mL (cps/mL).

Urine samples were taken at 1, 2, 3, 4, 5, 6, 7, 8 and 9 h using 20 GA 1.16IN (1.1 × 30 mm) endovenous catheters (BD Insyte-W™, Becton Dickinson Infusion Therapy Systems Inc., Utah, USA), as previously described.[15] Briefly, under Nembutal anesthesia, the animal was placed in dorsal recumbence. This endovenous catheter was passed through the urethra, first perpendicularly and then parallel to spinal cord. After urine collection, the radioactive contents of samples were measured for 1 min using a gamma counter. Data were expressed as %ID of radioactivity.

Pharmacokinetic analysis

After decay and background corrections, the radioactivity plasma concentration data (cps/mL) as a function of time was analyzed with the software program WinNonlin, Version 5.2 (Pharsight, Mountain View, CA, USA), by fitting on a non-compartmental model. The maximum concentration (C_{max}) of ^{123}I-Hyp, the time to reach C_{max} (t_{max}) and the half-life ($t_{1/2}$) were calculated. The elimination rate constant (kel) was estimated by a log-linear regression of radioactivity concentration data during the elimination phase. The terminal half-life ($t_{1/2Z}$) was calculated as 0.693/kel. The $AUC_{(t\text{-}0)}$ and the area under the first moment curve (AUMC) were determined using the linear/logarithmic trapezoidal rule with extrapolation ($AUC_{(0-\infty)}$, $AUMC_{(0-\infty)}$). From AUC and AUMC, mean residence time (MRT) was calculated. For quantification of urinary excretion, background- and decay-corrected time-activity curves were created from %ID values in urine and the $AUC_{(t\text{-}0)}$ were estimated. The estimated kinetic parameters were statistically compared between animals groups with and without catheter using GraphPad Prism (version 4.0; Graph Pad, San Diego, USA) by a paired Student's *t*-test. Quantitative data were expressed as mean ± SD. A *P* value of <0.05 was considered to be significant.

Metabolite analysis

Four hundred micro-liters of 2-h and 8-h samples of whole blood were collected. To obtain plasma, they were transferred to a VACUETTE® heparin tube and centrifuged at 3000 rpm for 5 min using a Centrifuge 4226 ALC. For proteins precipitation, 200 µL of the supernatant plasma was mixed with 300 µL of acetonitrile. After shaking the mixture vigorously for 30 s, it was allowed to stand for 3 min and then centrifuged at 3000 rpm for 5 min. The supernatant was filtered through disposable 0.22-µm-pore-size filters (GS, Millipore Corporation, Bedford, MA 01730) and 500 µL of 0.9% sodium chloride was added. Five hundred micro-liters of 2-h and 8-h samples of duodenal juices and urine (from animals with and without catheters) were centrifuged two times at 3000 rpm for 5 min. The pellets were discarded and the supernatants were filtered.

Aliquots of 200 µL of supernatant samples of plasma (serum), duodenal juices and urine were spiked with 5 µL of the 20 µg/mL solution of ^{127}I-Hyp. Next, they were analyzed by HPLC in a La Chrom. Elite Hitachi L-2130 pump system (Tokyo, Japan) equipped with an XTerra® C18 analytical column, 4.6 µm, 5 mm × 150 mm, a La Chrom Elite Hitachi L-2400 UV detector (Tokyo, Japan) at 254 nm and a Raytest radioactivity detector (Straubenhardt, Germany). A gradient mobile phase from 5 to 95 v/v acetonitrile in 0.05 M ammonium acetate buffer pH 7.0 was used at a flow rate of 1.0 mL/min. Fractions of 1.0 mL were collected with a model 2110 fraction collector (BIO-RAD laboratories, Richmond, CA, USA) and their radioactive contents were counted. Peak identification was performed by comparing the retention times of ^{123}I-Hyp and ^{127}I-Hyp, which was further analyzed by mass spectrometry (MS).

Gamma counting

After the duodenal fluid collection, animals with and without catheters were sacrificed by an intraperitoneal overdose of Nembutal. Organs (brain, thyroid, lungs, heart, liver, spleen, pancreas, stomach, small and large intestines, kidneys) and tissue samples (blood, bone, muscle) were removed post-mortem and counted for 1 min (cpm). The results were expressed as a %ID. Statistical data analysis was carried out using a paired t-test on the computer software GraphPad Prism version 5.00 for Windows. The values were expressed as mean ± standard deviation (SD). The significance of difference between groups was determined. The level of significance was established at $P < 0.05$.

Results

Radiolabelling

From HPLC analysis, Hyp was efficiently labeled with ^{123}I in a radiochemical yield higher than 95.0% and with a specific activity of about 1.0 GBq/µmol. A mixture consisting of radioiodinated Hyp ($\sim 1 \times 10^{-9}$ mol) without free iodine and unlabeled Hyp ($\sim 1.9 \times 10^{-6}$ mol) was formulated.

Figure 3 (upper case) shows a typical UV chromatogram. Unlabeled Hyp was detected having a retention time (RT) of 19.18 ± 0.15 min. A small peak at 20.91 ± 0.24 min was observed corresponding to the added ^{127}I-Hyp. Its mass spectra in negative mode revealed a unique fragment: accurate mass 628.9459 Da (found) and [M–H]-: 628.9739Da (theoretical). On the radiochromatogram, ^{123}I-Hyp eluted out at 22.13 ± 0.05 min (Figure 3 lower case).

The resulting ^{123}I-Hyp/unlabeled Hyp mixture was formulated at a concentration of 40 MBq/mL/1.9 mmol/L in DMSO/PEG400/PG/H_2O (25:25:25:25, v/v/v/v), as the solvent mixture. The final formulation appeared as a transparent red solution with no discernible aggregate formation.

Device design and catheterization procedure for biliary drainage

Foley catheters were successfully modified into a device to collect duodenal fluids in rats. The flexible silicone rubber catheter with a smooth tip could prevent perforation in the course of the catheterization through the thin-walled small luminal gastrointestinal system. During the catheter placement, all subjects survived the anesthesia, surgery and cannulation. No animals had to be excluded from the test due

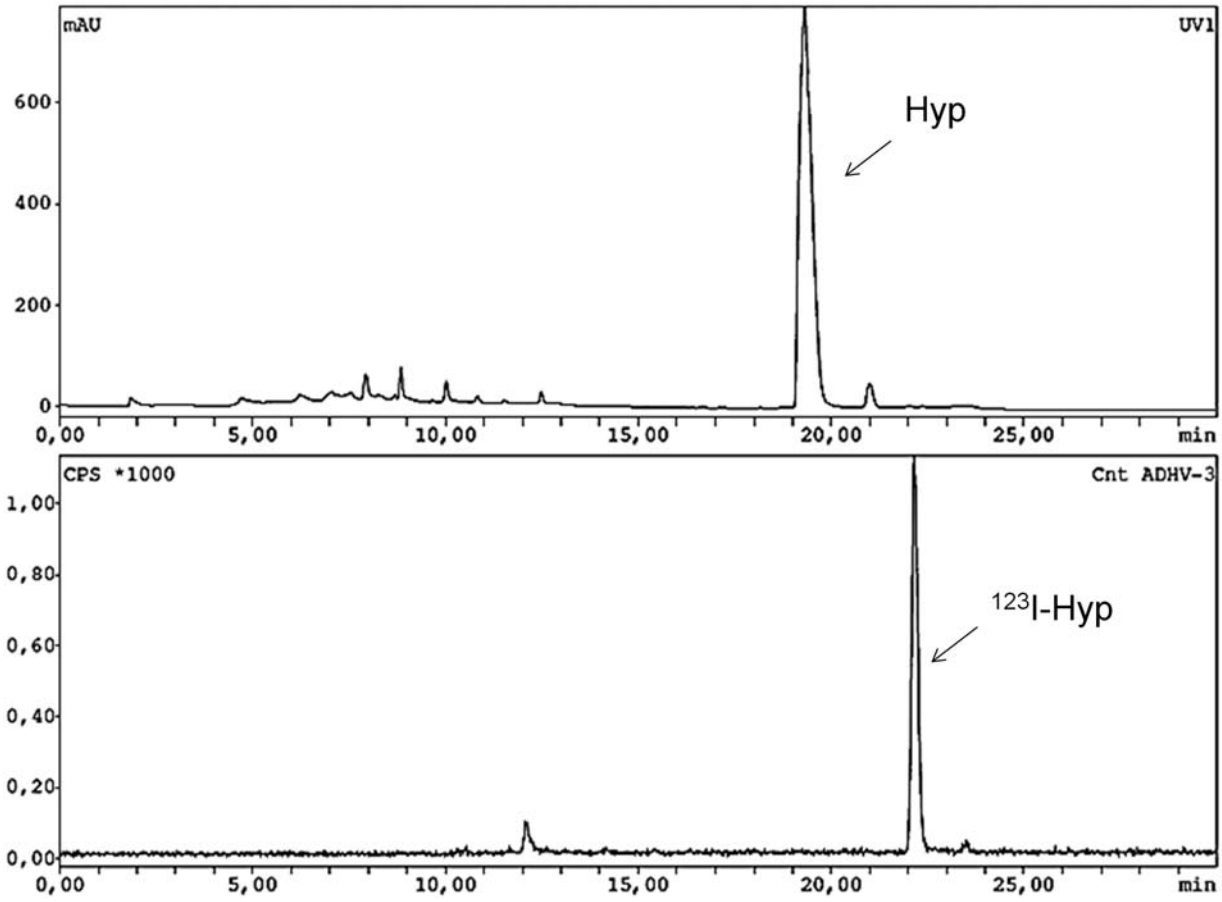

Figure 3 HPLC UV-chromatogram of unlabeled hypericin (Hyp) eluting at an RT of 19.18 ± 0.15 min (upper part) and HPLC radiochromatogram (lower part) of iodine-123-labeled hypericin (^{123}I-Hyp) with an RT of 22.13 ± 0.05 min

to procedural complications. Overall, the process turned out to be safe and took about 5 – 10 min for each animal.

Duodenal juice collection

The flow rate of duodenal juices ranged from 0.8 to 3.0 mL/h. The flow was fairly constant at 1.70 ± 0.39 mL/h over the first 6 h. However, in some animals subjected to cannulation for longer periods, it decreased to 0.8 mL/h during the successive 3 h. The total volumes of fluids collected varied from 3.5 to 5.0 mL and 8.0 to 12.0 mL during the 4 and 9 h, respectively.

Percentage of radioactivity excreted into the duodenal fluids over time

Figure 4a shows the profiles of the percentage of injected dose versus time in duodenal juice from catheterized rats at intervals of 0–4 h, 4–8 h and 20–24 h after ^{123}I-Hyp administration. Two peaks were observed within the first 8 h. The first peak reached the highest percentage (3.45 ± 0.26%) of the administered dose at 3 h. The second broader peak appeared at 8 h with a maximum value of 2.99 ± 0.32% that slowly declined until 21 h and rapidly dropped to 0.31 ± 0.01% during 22 and 24 h. Approximately 9.3% of the total dose was eliminated within the first 4 h, 5.1% between 4 and 8 h and 30.7% during 8 to 24 h. From AUC calculation, the radioactivity excreted into the duodenum within 24 h represented 45.69 ± 0.47% of the total administered dose.

Impact of the use of the catheter in the biological profile of ^{123}I-Hyp

Percentage of radioactivity excreted into the duodenal fluids over time. Figure 4b illustrates the percentage of radioactivity in duodenal juices within 9 h post ^{123}I-Hyp administration. A single bell-shaped curve was observed reaching maximum radioactivity (3.4 ± 0.18%) at 3 h followed by a slow exponential decay during the successive 6 h (1.69 ± 0.23% at 9 h). By AUC determination, within 9 h the total dose excreted into the duodenum accounted for 19.63 ± 0.58%.

Metabolite analysis in duodenal fluids. Representative radiochromatograms of 2-h and 8-h duodenal juices from animals with a catheter after a single IV administration of ^{123}I-Hyp are shown in Figure 4c and d. Results revealed a total of 5 radioactive peaks at 2 h and 8 h after ^{123}I-Hyp injection. The peak at the earliest RT of 2.53 ± 0.04 min corresponded to free iodine, which accounted for 11.49 ± 1.31% of the total radioactivity in duodenal juices. A predominant peak with an RT of 11.75 ± 0.39 min representing about 50%

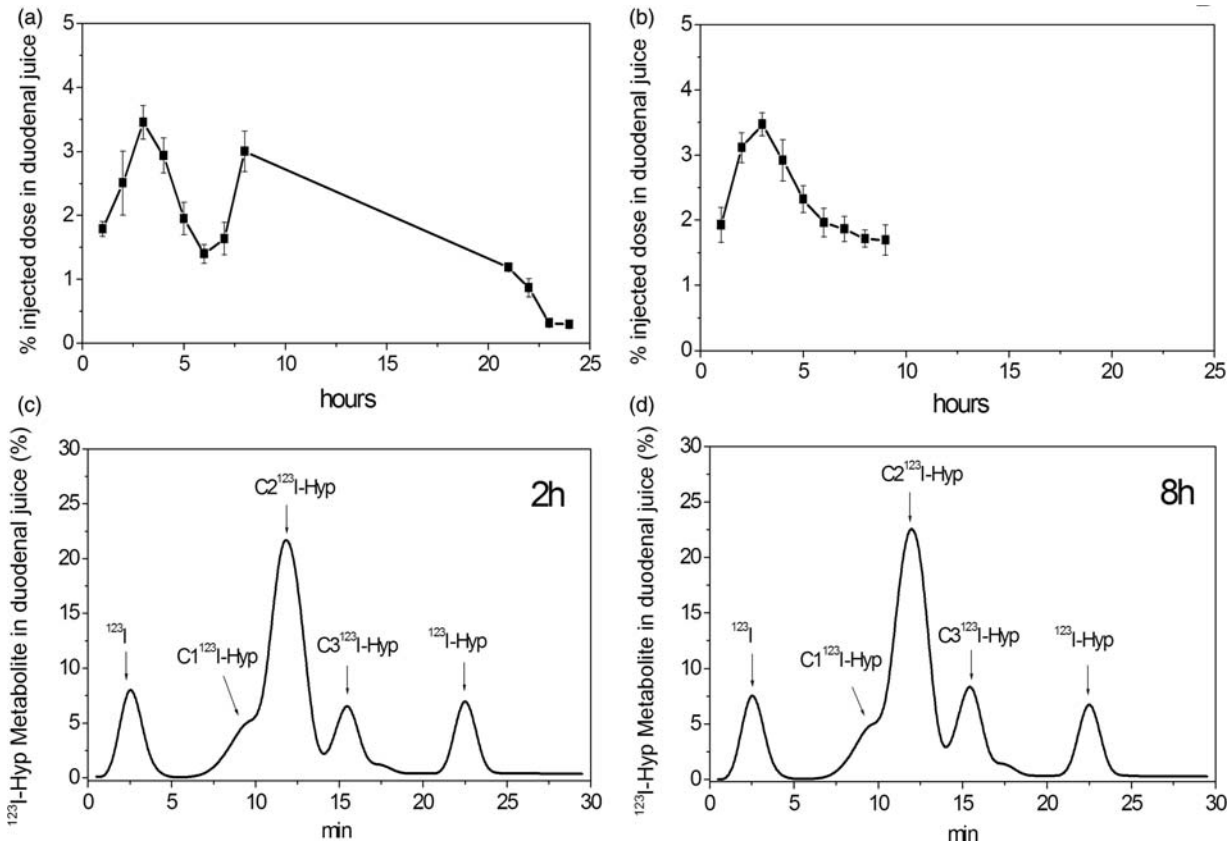

Figure 4 Excretion of intravenously injected ^{123}I-Hyp into duodenal juice and its radioactive metabolites. (a) Time-activity curves showing the percentage of injected dose of ^{123}I-Hyp in duodenal juices from rats with catheterization at intervals of 0–4, 4–8 and 8–24 h. Total radioactivity accounted for 46% in 24 h with two peaks at 3 h and 8 h, suggesting enterohepatic circulation. (b) Time-activity curves describing the percentage of injected dose of ^{123}I-Hyp in duodenal juices from rats with continuous catheterization for 9 h. A single peak representing about 20% of the administered dose was found. (c) Radio-chromatograms of ^{123}I-Hyp and its conjugated metabolites at 2 h after tracer injection. (d) Radio-chromatograms of ^{123}I-Hyp and its conjugated metabolites at 8 h after tracer injection. Similar patterns were observed (c vs. d). The peak at 2.53 min corresponded to free iodine accounting for 11.49% of the radioactivity. Radioiodinated Hyp in conjugated forms (C1-, C2- and C3-^{123}I-Hyp) appeared in three peaks at 9.53, 11.75, 15.55 min representing 60% of total peak area. Unchanged ^{123}I-Hyp accounting for 10.67% of the total counts eluted at 22.45 min. ^{123}I-Hyp: iodine-123-labeled hypericin

of total peak area was observed, overlapping with a smaller peak that came out at 9.53 ± 0.30 min. A fourth peak eluted out at 15.55 ± 0.08 min and contained 12.89 ± 1.51% of the total counts. The last peak representing 10.67 ± 0.15% of the biliary excretion corresponded to the unchanged ^{123}I-Hyp, which had an elution time of 22.45 ± 0.09 min like to that of the injected tracer (Figure 3 lower case), as confirmed by MS.

Plasma pharmacokinetics. Figure 5a illustrates the mean plasma concentrations as a function of time of the IV-administered ^{123}I-Hyp in animals with and without catheter. Overall, blood pool activity decayed exponentially by at least 40% during the first 3 h. Animals with catheters showed a marked decline in the last segment of the elimination curve with about 10% of radioactivity remaining in circulation at 9 h. Non-catheterized animals exhibited about 26% of the administered dose at this time point.

Pharmacokinetic parameters of the radioactive tracer in plasma specified with a non-compartmental model are summarized in Table 1. In non-catheterized group, a maximum concentration (C_{max}) of $3.98 \pm 0.2 \times 10^5$ cps/mL was reached in a maximum time (t_{max}) of 0.18 ± 0.02 h. The elimination rate constant (kel) accounted for $0.18 \pm 0.03\ h^{-1}$. The elimination half-life ($t_{1/2}$), terminal half-life ($t_{1/2z}$) and MRT were 4.20 ± 1.00 h, 24.7 ± 1.92 h and 35.13 ± 1.50 h, respectively. For the group with a catheter, a C_{max} of $0.92 \pm 0.03 \times 10^5$ cps/mL was reached in a t_{max} of 0.13 ± 0.04 h. The estimated value for kel was $0.33 \pm 0.07\ h^{-1}$. The values for $t_{1/2}$, $t_{1/2z}$ and MRT accounted for 2.10 ± 0.30, 3.78 ± 0.13 and 5.89 ± 0.03 h, respectively. By a two-tailed t-test, C_{max} and the area under the concentration time-curves from time zero to infinity ($AUC_{(0\text{-}\infty)}$) were significantly higher in non-catheterized than catheterized animals ($P = 0.001$). The catheterized group exhibited a lower MRT and $t_{1/2z}$ in comparison to the non-catheterized group ($P < 0.05$).

Metabolite analysis in plasma. No evidence of significant dehalogenation was detected by HPLC in both animal groups at 2 and 8 h after ^{123}I-Hyp injection (Figure 5b and c). At 2 h, there were two peaks in serum corresponding to free iodine and intact ^{123}I-Hyp with RT of 2.30 ± 0.40 min and 22.13 ± 0.05 min, respectively. The first small peak indicates the percentage of circulating iodine in the blood accounting for 1.56 ± 0.47%. The second major peak

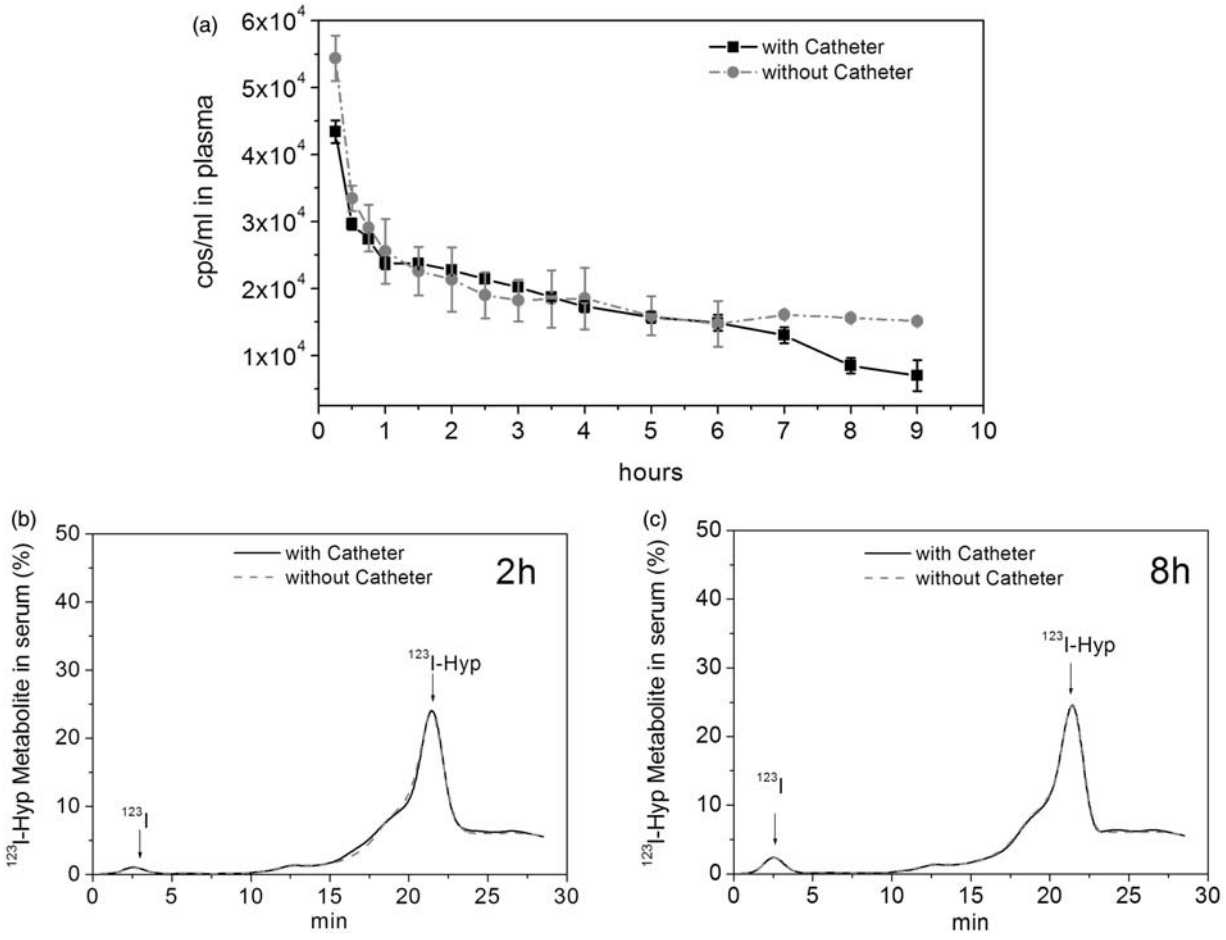

Figure 5 Distribution and elimination phase of intravenously administered ^{123}I-Hyp in plasma and its radioactive metabolites. (a) Plasma concentration-time curves of ^{123}I-Hyp in rats without and with catheter over 9 h. Plasma disappearance of radioactivity followed an exponential decay curve for the two groups. A faster terminal elimination phase was found in animals with catheter. (b) Radio-chromatograms of ^{123}I-Hyp and its conjugated metabolites in serum at 2 h after administration (c) Radio-chromatograms of ^{123}I-Hyp and its conjugated metabolites in serum at 8 h after administration. Similar patterns were observed at 2 h and 8 h. The two peaks at 2.30 min and 22.13 min corresponded to free iodine and intact ^{123}I-Hyp. Low percentages of free iodine were detected. ^{123}I-Hyp: iodine-123-labeled hypericin

Table 1 Pharmacokinetic parameters derived by non-compartmental modeling after intravenous administration of ^{123}I-Hyp in normal rats with and without catheter within 9 h post-injection

Parameter	Units	Without catheter (n = 5)	With catheter (n = 5)	*P* values
C_{max} ($\times 10^5$)	cps/mL	3.98 ± 0.22	0.92 ± 0.03	0.03
t_{max}	h	0.18 ± 0.02	0.13 ± 0.04	0.06
$t_{1/2}$	h	4.70 ± 1.00	2.10 ± 0.30	0.14
Kel	1/h	0.18 ± 0.03	0.33 ± 0.07	0.04
$t_{1/2z}$	h	24.7 ± 1.92	3.78 ± 0.13	0.02
$AUC_{(0-t)}$ ($\times 10^5$)	cps/mL/h	1.65 ± 0.17	1.51 ± 0.10	0.21
$AUC_{(0-\infty)}$ ($\times 10^5$)	cps/mL/h	7.04 ± 0.04	1.90 ± 0.43	0.001
$AUMC_{(0-\infty)}$ ($\times 10^6$)	cps/mL/h^2	24.72 ± 0.90	1.12 ± 0.41	0.001
MRT	h	35.13 ± 1.50	5.89 ± 0.03	0.04

The values are expressed as mean ± standard deviation.
Differences between groups are considered significant at $P < 0.05$.

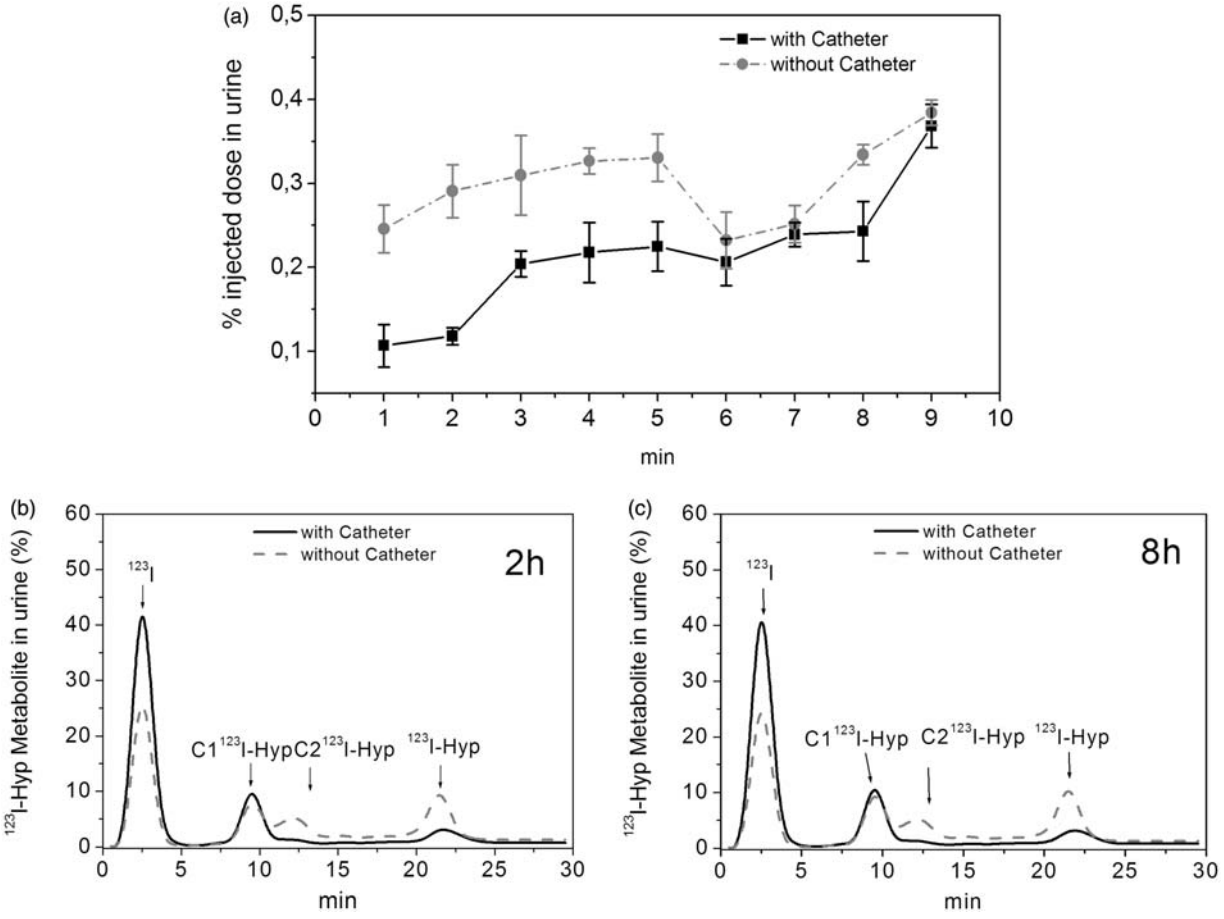

Figure 6 Urinary excretion of ^{123}I-Hyp and its radioactive metabolites. (a) Time-activity curves showing the percentage of injected dose of ^{123}I-Hyp in urine from rats without and with catheter for 9 h. Low levels of radioactivity were found in both groups. Animals without catheter exhibited higher urinary elimination. (b) Radio-chromatograms of ^{123}I-Hyp and its conjugated metabolites in urine at 2 h. (c) Radio-chromatograms of ^{123}I-Hyp and its conjugated metabolites in urine at 8 h. Similar compositions were observed at 2 h and 8 h after tracer injection. Free iodine eluting at 2.60 min represented the highest percentages of excreted radioactivity (>40%). Unchanged ^{123}I-Hyp came out at 22.0 min. In non-catheterized animals, ^{123}I-Hyp in conjugated forms (C1- and C2-^{123}I-Hyp) were observed at 9.56 and 11.90 min. Lower percentages of unchanged ^{123}I-Hyp and no C1-^{123}I-Hyp were found in catheterized group. ^{123}I-Hyp: iodine-123-labeled hypericin

(98.48 ± 1.64%) representing ^{123}I-Hyp had an elution time identical to that of the injected ^{123}I-Hyp (Figure 3), as proven by MS. At 8 h, a small increase in free iodine level (3.41 ± 0.80%) was observed for the two groups.

Urine pharmacokinetics. Areas under the urinary excretion curves (AUC_{0-t}) in rats with and without catheters are shown in Figure 6a. Low but slowly increasing levels of radioactivity (<2.0%) were found in the urine for the two groups. Overall, the radioactivity excretion was higher in animals without the catheter than in those with it. Statistical analysis of AUC_{0-t} revealed significant differences between catheterized (1.485%) and non-catheterized animals (1.981%) ($P = 0.019$).

Metabolite analysis in urine. HPLC analysis of 2-h and 8-h urine samples from both groups showed differences regarding the metabolite percentages and composition (Figure 6b and c). In the catheter group, a total of four radioactive peaks including one for ^{123}I-Hyp were detected. The first major peak with an RT of 2.60 ± 0.10 min reaching 39.37 ± 1.45% of the radioactivity urinary excretion corresponded to free iodine. Two overlapped peaks, each one accounting for about 12%, were observed with RT of 9.56 ± 0.72 min and 11.90 ± 0.84 min. The last peak with a RT of 22.0 ± 0.5 min and 20.74 ± 1.93% of the total radioactivity in urine corresponded to ^{123}I-Hyp. Whereas, in catheterized animals, only three radioactive peaks were seen. The main peak of free iodine with RT of 2.18 ± 0.95 min was detected reaching 65.04 ± 2.78% of the urinary radioactivity. A second small peak coming out at 9.55 ± 0.86 min represented 15.09 ± 1.94%. The latest peak corresponding to ^{123}I-Hyp had an RT of 22.01 ± 0.52 min and represented 8.47 ± 1.86% of the counts in urine, as confirmed by MS.

Biodistribution. The results of the tissue distribution of ^{123}I-Hyp in percentage of injected dose per organ (%ID) in rats with and without catheter at 9 h are summarized in Table 2.

The distribution patterns of ^{123}I-Hyp in both groups were rather similar. The radioactivity uptakes in most

Table 2 Tissue distribution of ^{123}I-Hyp in normal rats with and without catheter at 9 h post-injection

	%ID per organ		
	Without catheter (n = 5)	With catheter (n = 5)	*P* values
Blood	17.79 ± 2.44	14.79 ± 1.93	0.73
Brain	0.09 ± 0.02	0.08 ± 0.03	0.78
Thyroid	0.39 ± 0.14	0.51 ± 0.03	0.34
Lungs	4.34 ± 0.18	3.40 ± 0.73	0.24
Heart	0.49 ± 0.01	1.25 ± 0.38	0.11
Liver	19.42 ± 2.20	12.26 ± 1.88	0.04[a]
Spleen	3.87 ± 0.82	3.89 ± 0.19	0.98
Pancreas	0.33 ± 0.07	0.39 ± 0.02	0.32
Stomach	4.52 ± 0.61	5.66 ± 2.24	0.56
Small intestines	18.95 ± 4.32	1.82 ± 0.41	0.01[a]
Large intestines	2.62 ± 0.19	1.59 ± 0.07	0.04[a]
Kidneys	2.52 ± 0.12	2.63 ± 0.01	0.83
Muscle	14.48 ± 0.71	14.19 ± 3.53	0.92
Bone	11.70 ± 1.30	12.42 ± 2.81	0.35

The values are expressed as mean ± standard deviation.
[a]Differences between groups are considered statistically significant at $P < 0.05$.

tissues were not significantly different ($P > 0.05$). The proportion of injected dose (%ID) was substantially high in the blood (>14%ID). The organs that retained the highest levels of radioactivity were the intestines, followed by the liver, stomach, spleen and lungs. The lowest tracer uptake (<1.0%ID) was found in the brain and pancreas. Bone and muscle showed a high amount (>12.0%ID) due to their relatively large total masses. Regarding the dissimilarities between the groups, there were statistically significant differences in radioactivity accumulation in the intestines and liver. Above all, animals without a catheter exhibited extremely higher values in the small intestines (18.95 ± 4.32 %ID) than animals with a catheter (1.82 ± 0.41%) ($P = 0.01$). Blood and lungs also retained a greater percentage of the total activity administered.

Discussion

Radiodiodinated hypericin (^{131}I-Hyp) is an attractive necrosis avid agent for complementary cancer therapy after a necrosis inducing treatment. Because of its high lipophilicity with an octanol-water partition coefficient (log P) value (3.08 ± 0.03)[11] and molecular size greater than 300 g/mol[16], ^{131}I-Hyp is not readily eliminated by the kidneys. The persistently high levels of radioactivity observed accumulating in intestines suggested that the excretion of ^{131}I-Hyp was predominantly hepatobiliary, which may impose real concerns of irradiation overexposure and subsequent acute gastrointestinal syndrome. Damage to intestinal crypt mucosal cells can promote a progressive epithelial denudation, leading to mucosal collapse and intestinal ulceration.[17,18]

Thus, we designed this study to investigate the feasibility of using a device in cancer patients undergoing OncoCiDia for the drainage of the radioactive wastes released into the intestines. Drainage catheters in different sizes, materials and types depending on the specific needs of the patient have been widely used in the clinic.[19–22] In this study, we developed a transoral duodenal balloon catheter for rats by the modification of a human Foley urinary catheter. However, because the drainage apertures were placed in the portion of the duodenum distal to the sphincter of Oddi, the collected fluid was not pure bile but rather a mixture of biliary, pancreatic and gastric secretions. In the clinic, a nasobiliary drainage catheter can alternatively be applied during an endoscopic retrograde cholangiopancreatography (ERCP) procedure to more selectively aspirate bile excretion, though this is more technically demanding. Experimentally, to determine the fraction of the total dose administered that is secreted into the intestines; we preferred to express the results as a %ID rather than %ID per gram.

Although OncoCidia is intended for cancer treatment by using ^{131}I-Hyp after a VDA attack, Hyp was herein labeled with the gamma emitter ^{123}I to minimize the radiation overexposure. Since isotopes share identical chemical and biological properties, both ^{123}I and ^{131}I can volatilize and be trapped into the body through inhalation after contamination. Eventually, they accumulate in the thyroid gland, which is the critical target organ for exposure, particularly for the beta-emitter ^{131}I. There, it will be retained with a biologic half-life of 120 days, so any ^{131}I will decay before being excreted, causing the irradiation effect. Moreover, because radiopharmaceutical chemistry uses very small amounts of compound that might be difficult to accurately detect in biological samples, Hyp was also labeled with the stable non-radioactive ^{127}I. By doing so, the presence of intact ^{123}I-Hyp either in solution or biological medium was identified by sample spiking with the non-radioactive ^{127}I-Hyp that gives a molecule with distinctive molecular size by MS. On HPLC, the intact ^{123}I-Hyp and the added ^{127}I-Hyp were then matched in terms of retention times in radiometric and UV channels, respectively.

Based on previous studies about biodistribution of $^{123/131}$I-Hyp,[8,9] it has been found the radioactivity is cleared from most of the normal organs and then accumulated into intestines within the first day after injection. A maximum time interval of 24 h was then defined for duodenal collection in the first part of this study.

As expected, nearly 45% of the dose administered was excreted via the bile into the bowel within 24 h, which could be removed by using the catheter. This study confirms earlier reports that suggested the hepatobiliary pathway is a major excretion route of radioiodinated Hyp.[7,12,13] However, the time-activity curves showed the presence of double peaks of radioactivity within 8 h after ^{123}I-Hyp administration. The first peak most likely characterizes the typical elimination route of ^{123}I-Hyp via bile, which occurred a few hours after injection. However, the second peak appearing in the duodenal juices from animals drained between 4 and 8 h after ^{123}I-Hyp injection might be related to the enterohepatic circulation (EHC) of ^{123}I-Hyp and its metabolites. It is important to notice that these animals had received the radioactive dose 4 h before

catheterization and fluid drainage. During that period, once ^{123}I-Hyp was excreted into the bile, it underwent some degree of reabsorption along the gastrointestinal tract. It then returned to the liver through the portal circulation, prolonging the time of its elimination from the body. This may explain the appearance of the secondary peak in the duodenal contents.

As earlier studies have shown the EHC effects on the absorption, distribution, metabolism and excretion of other systemically administered drugs with marked lipophilicity as ^{123}I-Hyp,[23–25] a second protocol was designed for better understanding the processes involved in the hepatic excretion and reabsorption of ^{123}I-Hyp. By using the new catheter to collect the duodenal juice and disrupt the EHC, we explored the pharmacokinetic and biodistribution of ^{123}I-Hyp in animals for 9 h without EHC. Such a collection period was selected for two reasons. First, it covers the two peaks observed in the initial protocol. Second, it was noticed that a longer period of cannulation may cause a decrease in the flow rate of drainage. Results from time-activity curves show a single peak of radioactivity with a maximum value within the first 4 h. It seems that the continuous fluid drainage prevented the EHC of ^{123}I-Hyp and the secondary radioactive peak.[26]

Animals without catheters but with intact EHC indeed differed. The effects of the EHC of ^{123}I-Hyp were clearly represented by the pharmacokinetic parameters. They exhibited delayed excretion of ^{123}I-Hyp, mainly during the terminal phase. In general, we observed a higher C_{max} and area under the plasma concentration versus time curves (AUC); extended residence time (MRT) and plasma half-life ($t_{1/2}$) as well as reduced elimination rate constant (kel). Some of these values are similar to those reported for Hyp or its iodinated derivatives in animals with intact EHC.[27,28] In addition, these findings are in agreement with previous studies regarding the role of EHC in the biological profile of other drugs. For instance, a review about EHC and its physiological, pharmacokinetic and clinical implications indicates that the cycling is associated with a longer apparent half-life in a plasma concentration-time profile.[25] A study on pharmacokinetic modeling for EHC in Rhesus monkeys showed that EHC can lead to a change in pharmacokinetic properties, such as extended half-life ($t_{1/2}$) and increased plasma exposure (AUC).[29]

However, discrepancies regarding EHC do exist in the literature. Some studies clearly showed the appearance of multiple peaks,[30,31] while others reported smooth curves with a single peak.[32–34] But with ^{123}I-Hyp, we believe once re-absorbed from intestines, it is rapidly and constantly taken up by hepatocytes. Thus, it is difficult to detect secondary peaks of radioactivity in the blood circulation, unlike the two peaks in the bile observed when the EHC was possible.

Another interesting finding was the characters of radioactive components. Duodenal juice and urine showed distinctive metabolites within the whole experiment period (8 h). In duodenal juice, the major quantities of radioactivity were either in conjugated or unchanged ^{123}I-Hyp form. In particular, the conjugated form reached the highest percentages of the total peak area (>60%). Since one of the major bile components is cholesterol, that undergoes hepatobiliary elimination into the intestines where it is reabsorbed in about 50% into the bloodstream,[35] and since recent evidence has shown the preferential binding between cholesterol and Hyp,[36,37] it might be possible that cholesterol and ^{123}I-Hyp form complexes in their initial passage through the liver. This may also contribute to the EHC of ^{123}I-Hyp. However, both cholesterol and ^{123}I-Hyp are highly lipophilic with poor water solubility. But, during the metabolite analysis the ^{123}I-Hyp conjugates appeared to be less lipophilic, as proven by their shorter retention times, wherein bile salts may play a role. Given the relatively large molecular size of ^{123}I-Hyp (628 g/mol) and its chemical structure, another possibility is the hepatic glucuronidation of ^{123}I-Hyp, in which it is conjugated to glucuronic acid and subsequently excreted into bile.[38,39] The resulting glucuronides are normally more soluble than the parental non-glucuronidated compound, which may explain their faster elution from the hydrophobic HPLC column in comparison to ^{123}I-Hyp.

In the serum, no differences were observed between the two groups. The high radiochemical purity of the tracer before injection and the low levels of circulating iodine over time indicated the *in vivo* stability of the carbon-radiohalogen bond of ^{123}I-Hyp. Persistent low urinary excretion of ^{123}I-radioactivity was identified in both groups. Overall, the metabolic pattern in urine was characterized for the presence of large percentages of free iodine. ^{123}I-Hyp either in conjugated or unchanged form was also observed in much smaller amounts. As expected, in catheterized animals, urinary elimination of ^{123}I-radioactivity was reduced due to the duodenal drainage. By using the catheter, the radioactive juices in intestinal tract, which otherwise would be re-absorbed into the blood, are removed from the body, consequently reducing the radioactivity percentage excreted via urine.

Tissue biodistribution of ^{123}I-Hyp was also influenced by the use of the catheter. Comparing tissue uptake between the two groups showed striking differences in the total radioactivity retained in the intestines, which was previously identified as the dose-limiting organ. By using this device, the percentage dose per organ in the small intestines was decreased by 10 times, which was comparable to those of other organs (e.g. heart, kidneys) that typically showed a low accumulation of the tracer. This result highly indicates that bile drainage can serve as a safety measure for OncoCiDia. However, further dosimetry studies have to be done for accurately evaluating the impact of the use of the duodenal drainage catheter to the overall systemic exposure of ^{131}I-Hyp.

Despite the duodenal drainage catheter helped minimize the overall systemic exposure of ^{131}I-Hyp, whether it could influence the affinity of ^{131}I-Hyp to necrosis remains unclear. However, based on our observations, it would be unlikely. First, the majority of excreted ^{123}I-Hyp molecules will not be absorbed but be slowly eliminated via faces. Secondly, those ^{123}I-Hyp molecules, once excreted into the guts, might be deiodinated by the intestinal enzymes and absorbed as free ^{123}I and Hyp or its metabolites, which will

not affect the affinity/uptake of ^{123}I-Hyp as such to necrotic tissues. Third, even if some fraction of intact ^{123}I-Hyp could be absorbed, it will remain in the EH circulation (not blood circulation) due to the excessive hepatocytic capacity for handling ^{123}I-Hyp.

In conclusion, the duodenal catheterization and drainage described in this report proves to be feasible in rats, which offer another method to evaluate biliary excretion of the drugs in rodents. The potential clinical usefulness of this approach is also clearly evidenced for therapies such as OncoCiDia, where the bile-excreted drug and/or metabolites are unwanted and harmful.

Author contributions: Guarantor of integrity of entire study, NY, VA, OR; study concepts/study design or data acquisition or data analysis/ interpretation, all authors; manuscript drafting or manuscript revision for important intellectual content, all authors; approval of final version of submitted manuscript, all authors; literature research, CMM, FY, VA, OR, NY; experimental studies, CMM, FY, NY; statistical analysis, CMM, FY, NY and manuscript editing, CMM, NY.

ACKNOWLEDGEMENT

This study has been supported in part by the KU Leuven Molecular Small Animal Imaging Center MoSAIC (KUL EF/05/08) and the center of excellence *in vivo* molecular imaging research (IMIR); KU Leuven projects IOF-HB/08/009 and IOF-HB/12/018; the European Union (Asia-Link CfP 2006-EuropeAid/123738/C/ACT/Multi-Proposal No. 128-498/111), the National Natural Science Foundation of China (81071828), and Jiangsu Province Natural Science Foundation (BK2010594). The corresponding author is currently a Bayer Lecture Chair holder.

REFERENCES

1. Katholieke Universiteit Leuven-Oncocidia. http://vimeo.com/44871398 (accessed 29 June 2013)
2. Thorpe PE. Vascular targeting agents as cancer therapeutics. *Clin Cancer Res* 2004;**10**:415–27
3. Ni Y, Chen F, Sun XH, De Keyzer F, Jie Y, Vandecaveye V, Marchal G. Monitoring tumorocidal effects of a vascular targeting agent using multiparametric MR in a rodent liver tumor model. *Scientific Assembly and Annual Meeting of Radiological Society of North America*. 2006; Abstract No. LL-GI2198-H07
4. Draves AH, Walker SE. Analysis of the hypericin and pseudohypericin content of commercially available St John's Wort preparations. *Can J Clin Pharmacol* 2003;**10**:114–8
5. Olivo M, Du HY, Bay BH. Hypericin lights up the way for the potential treatment of nasopharyngeal cancer by photodynamic therapy. *Curr Clin Pharmacol* 2006;**1**:217–22
6. Ni Y, Bormans G, Marchal G, Verbruggen A. Necrosis avid tracer agent. European Patent EP 1 651 201 B1, July 25, 2003
7. Fonge HA, Bormans G, Ni Y, Chen F, Verbeke K, Marchal G, Mortelmans L, Verbruggen A. Evaluation of mono-I-123- Hypericin as necrosis avid tracer agent. *Eur J Nucl Med Mol Imaging* 2004;**31**:S381
8. Li J, Sun Z, Zhang J, Shao H, Cona MM, Wang H, Marysael T, Chen F, Prinsen K, Zhou L, Huang D, Nuyts J, Yu J, Meng B, Bormans G, Fang Z, de Witte P, Li Y, Verbruggen A, Wang X, Mortelmans L, Xu K, Marchal G, Ni Y. A dual-targeting anticancer approach: soil and seed principle. *Radiology* 2011;**260**:799–807
9. Cona MM, Alpizar YA, Li J, Bauwens M, Feng Y, Sun Z, Zhang J, Chen F, Talavera K, de Witte P, Verbruggen A, Oyen R, Ni Y. Radioiodinated hypericin: its biodistribution, necrosis avidity and therapeutic efficacy are influenced by formulation. *Pharm Res* 2013 [Epub ahead of print]
10. Li J, Cona MM, Chen F, Feng Y, Zhou L, Zhang G, Nuyts J, de Witte P, Zhang J, Yu J, Oyen R, Verbruggen A, Ni Y. Sequential systemic administrations of combretastatin A4 phosphate and radioiodinated hypericin exert synergistic targeted theranostic effects with prolonged survival on SCID mice carrying bifocal tumor xenografts. *Theranostics* 2013;**3**:127–37
11. Stone HB, Coleman CN, Anscher MS, McBride WH. Effects of radiation on normal tissue: consequences and mechanisms. *Lancet Oncol* 2003;**4**:529–36
12. Bormans G, Huyghe D, Christiaen A, Verbeke K, de Groot T, Vanbilloen H, de Witte P, Verbruggen A. Preparation, analysis and biodistribution in mice of iodine-123 labelled derivatives of hypericin. *J Label Compd Radiopharm* 2004;**47**:191–8
13. Fonge H, Jin L, Wang H, Ni Y, Bormans G, Verbruggen A. Synthesis and preliminary evaluation of mono-[^{123}I]iodohypericin monocarboxylic acid as a necrosis avid imaging agent. *Bioorg Med Chem Lett* 2007;**17**:4001–5
14. Van Landeghem L, Blue RE, Dehmer JJ, Henning SJ, Helmrath MA, Lund PK. Localized intestinal radiation and liquid diet enhance survival and permit evaluation of long-term intestinal responses to high dose radiation in mice. *PLoS ONE* 2012;**7**:e51310
15. Oliveira PA, Pires MJ, Nóbrega C, Arantes-Rodrigues R, Calado AM, Carrola J, Ginja M, Colaço A. Technical report: technique of bladder catheterization in female mice and rats for intravesical instillation in models of bladder cancer. *Scand J Lab Anim Sci* 2009;**36**:5–9
16. Drug Excretion. Biliary excretion. http://www.merckmanuals.com/professional/clinical_pharmacology/pharmacokinetics/drug_excretion.html (accessed 21 June 2013)
17. Donnelly EH, Nemhauser JB, Smith JM, Kazzi ZN, Farfán EB, Chang AS, Naeem SF. Acute radiation syndrome: assessment and management. *South Med J* 2010;**103**:541–6
18. Bertho JM, Griffiths NM, Gourmelon P. The medical diagnosis and treatment of radiation eve exposed people. Eleventh Congress of the International Radiation Protection Association, Madrid. Spain, 2004
19. Widmann WD, Diehl W, Edoga JK, McLean ER Jr. An improved double-lumen biliary catheter for cholangiography. *Am J Surg* 1967;**154**:317–9
20. Thorbjarnarson B. A catheter for controlled biliary drainage. *Arch Surg* 1987;**95**:946–7
21. Tamada K, Wada S, Tomiyama T, Ohashi A, Satoh Y, Miyata T, Higashizawa T, Gotoh Y, Ido K, Sugano K. Percutaneous recanalization of the bile duct along an endoscopic naso-biliary catheter. *J Gastroenterol* 2000;**35**:622–6
22. Daglilar ES, Yoon WJ, Mino-Kenudson M, Brugge WR. Controlled swine bile duct ablation with a bipolar radiofrequency catheter. *Gastrointest Endosc* 2013;**77**:815–9
23. Jandacek RJ, Tso P. Enterohepatic circulation of organochlorine compounds: a site for nutritional intervention. *J Nutr Biochem* 2007;**18**:163–7
24. Jaggi R, Addison RS, King AR, Suthers BD, Dickinson RG. Conjugation of desmethylnaproxen in the rat–a novel acyl glucuronide-sulfate diconjugate as a major biliary metabolite. *Drug Metab Dispos* 2002;**30**:161–6
25. Roberts MS, Magnusson BM, Burczynski FJ, Weiss M. Enterohepatic circulation: physiological, pharmacokinetic and clinical implications. *Clin Pharmacokinet* 2002;**41**:751–90
26. Ghibellini G, Leslie EM, Brouwer KL. Methods to evaluate biliary excretion of drugs in humans: an updated review. *Mol Pharm* 2006;**3**:198–211
27. Kong M, Zhang J, Jiang C, Jiang X, Li Y, Gao M, Yao N, Huang D, Wang X, Fang Z, Liu W, Sun Z, Ni Y. Necrosis affinity evaluation of ^{131}I-hypericin in a rat model of induced necrosis. *J Drug Target* 2013 [Epub ahead of print]
28. European Medicines Agency evaluation of Medicines for Human Use. Doc. Ref.: EMA/HMPC/101304/2008, London, 2009
29. Shou M, Lu W, Kari PH, Xiang C, Liang Y, Lu P, Cui D, Emary WB, Michel KB, Adelsberger JK, Brunner JE, Rodrigues AD. Population

pharmacokinetic modelling for enterohepatic recirculation in Rhesus monkey. *Eur J Pharm Sci* 2005;**26**:151–61
30. Jeong H, Kaplan B. Therapeutic monitoring of mycophenolate mofetil. *Clin J Am Soc Nephrol* 2007;**2**:184–91
31. Naidoo V, Mulders MS, Swan GE. The intravenous pharmacokinetics of diminazene in healthy dogs. *J S Afr Vet Assoc* 2009;**80**:215–9
32. Takamatsu N, Welage LS, Hayashi Y, Yamamoto R, Barnett JL, Shah VP, Lesko LJ, Ramachandran C, Amidon GL. Variability in cimetidine absorption and plasma double peaks following oral administration in the fasted state in humans: correlation with antral gastric motility. *Eur J Pharm Biopharm* 2002;**53**:37–47
33. Wang Y, Roy A, Sun L, Lau CE. A double-peak phenomenon in the pharmacokinetics of alprazolam after oral administration. *Drug Metab Dispos* 1999;**27**:855–9
34. Königsson K, Törneke K, Engeland IV, Odensvik K, Kindahl H. Pharmacokinetics and pharmacodynamic effects of flunixin after intravenous, intramuscular and oral administration to dairy goats. *Acta Vet Scand* 2003;**44**:153–9
35. Bergstrom S. *CIBA Foundation Symposium on Biosynthesis of Terpenes and Sterols*. Boston: Little, Brown and Co., 1959, p. 185
36. Ho YF, Wu MH, Cheng BH, Chen YW, Shih MC. Lipid-mediated preferential localization of hypericin in lipid membranes. *Biochim Biophys Acta* 2009;**1788**:1287–95
37. Eriksson ESE, Eriksson LA. The influence of cholesterol on the properties and permeability of hypericin derivatives in lipid membranes. *J Chem Theory Comput* 2011;**7**:560–74
38. Barceloux DG. *Medical toxicology of natural substances: foods, fungi, medicinal herbs, plants, and venomous animals*. New York: John Wiley & Sons, Inc., 2008, p. 90
39. Kerb R, Brockmöller J, Staffeldt B, Ploch M, Roots I. Single-dose and steady-state pharmacokinetics of hypericin and pseudohypericin. *Antimicrob Agents Chemother* 1996;**40**:2087–93

(Received July 8, 2013, Accepted September 9, 2013)